Available online at www.sciencedirect.com
ScienceDirect
Trans. Nonferrous Met. Soc. China 24(2014) 100−107
Transactions of Nonferrous Metals Society of China
www.tnmsc.cn

# Dual motion fretting wear behaviors of titanium and its alloy in artificial saliva

Bao-rong ZHANG[1,2], Zhen-bing CAI[3], Xue-qi GAN[1], Min-hao ZHU[3], Hai-yang YU[1]

1. State Key Laboratory of Oral Diseases, Sichuan University, Chengdu 610041, China;
2. Department of Stomatology, Aviation General Hospital, Beijing 100012, China;
3. Tribology Research Institute, Key Laboratory for Advanced Materials Technology of Ministry of Education, Southwest Jiaotong University, Chengdu 610031, China

Received 6 November 2012; accepted 8 July 2013

**Abstract:** A dual motion combined by radial and tangential fretting was achieved on a modified hydraulic fretting wear test rig. The dual motion fretting tests of medical pure titanium (TA2) and Ti6Al7Nb alloy in artificial saliva were carried out under varied contact inclined angles (45° and 60°), and the maximum imposed load varied from 200 to 400 N at a constant loading speed of 6 mm/min. The effects of the cyclic vertical force and the inclined angle were investigated in detail. Dynamic analysis in combination with microscopic examinations shows that the wear scar and plastic deformation accumulation present a strong asymmetry. The Ti6Al7Nb has better wear resistance than TA2 in artificial saliva at the same test parameters, and with the increase of inclined angle and decrease of imposed load, the wear reduces accordingly. The wear mechanisms of pure titanium TA2 and Ti6Al7Nb alloy under the condition of dual motion fretting in artificial saliva are abrasive wear, oxidative wear and delamination.
**Key words:** titanium alloy; fretting wear; dual motion fretting; tangential fretting; radial fretting; wear mechanism

## 1 Introduction

Abutment screw fracture and loosening of single and multiple fixed partial prostheses attached to external hexagonal implants are commonly encountered [1,2]. The service life of the metal devices depends upon two factors, ie, the mechanical and environmental factors, the reduction of wear under fretting corrosion [3−7]. In dental implants, fretting motion is induced by the biting force, mastication on the implant/abutment or on the abutment/ceramic crown [8]. Fretting damage would lead to toxicity, reddening and allergic reactions of the skin, inflammation of tissues.

Therefore, just as the degree of implant integration with surrounding osseous tissue is paramount to physiologic success, the degree of mechanical integration within the prosthodontic interfaces is crucial to prosthodontic success [9]. A 3-year evaluation of 16 patients with 23 single-tooth implants revealed that 57% of the abutment screws became unstable in the first year, 30% of those became unstable in the second year, and 5% of those became unstable in the third year. Only 35% of the abutment screws remained stable throughout the entire follow-up period [10].

To understand how screw loosening can occur, it is necessary to understand certain mechanical damage principles. The abutment screw and implant are joined together by the dentist to form a clamped joint. When the screw is first tightened, an initial tensile preload is generated within the screw. The ultimate effect of this preload is to place the abutment/implant assembly in compression, which will result in friction (fretting) between the screw and implant thread, the head of the screw and the abutment [11]. During the human physical activity, the normal thresholds for micro-movements at the screw−implant thread interface are very small. Those movements at the interface are hardly detectable in vivo, but fretting damages of the interface should be induced and finally cause the initial failures for the accumulation of mico-cracks and other damages [12]. Therefore, evaluation of the fretting wear behaviors of the screw−implant thread interface is very important in their application.

**Foundation item:** Project (81170996) supported by the National Natural Science Foundation of China
**Corresponding author:** YU Hai-yang; Tel: +86-28-87797838; E-mail: yhyang6821@scu.edu.cn
DOI: 10.1016/S1003-6326(14)63033-8

There have been considerable interests in the experimental and theoretical studies on fretting behavior under various conditions. Under the contact of ball-on-flat, there are only 4 basic fretting modes, such as reciprocating or tangential, radial, rotational and torsional modes [13]. In particular, the tangential mode has been widely investigated. However, for many fretting cases in real life applications, relative motion of fretting is very complex and the damage is often induced by combined fretting modes with a superimposition of two or more in the 4 basic modes. As shown in Fig. 1(a), the fretting occurring at the screw helicoid of dental implants always combines the tangential and radial fretting modes.

Titanium and its alloys are widely used as implant materials because of their low density, good intensity, relatively low elastic modulus, excellent biocompatibility and corrosion resistance [14,15]. In this work, the complex fretting wear behaviors combined by the tangential and radial fretting modes of titanium alloy in artificial saliva of 37 °C (body temperature) in a fretting test system are studied in detail. The aim of this investigation is focused on the dual motion fretting running behaviors and its mechanisms of titanium alloy in body simulation environments.

## 2 Experimental

A ball-on-flat contact configuration was selected as the friction test mode. The surface of flat specimens was inclined to the horizontal direction, as shown in Fig. 1(b) [16]. Two upper clamps with the inclined angles $\theta$ of 45° and 60° were manufactured for the varied tests. Cyclic displacement between contact surfaces was measured by the extensometer. Variations of vertical force versus displacement ($F$−$D$ curve) of dual motion fretting were recorded as a function of cycles. The displacement and force measured from the $F$−$D$ curves were not real values of displacement and frictional force at the interface in the case of tangential fretting. Under an extreme condition, when $\theta$=90°, the fretting contact situation turned to radial fretting mode; and when $\theta$=0°, the tangential fretting mode could be obtained.

The Ti6Al4V ball with a diameter of 40 mm was used (HV 345, $R_a$=0.05 μm). The flat specimens with dimensions of 10 mm×10 mm×20 mm were machined from the pure titanium (TA2) and two medical titanium alloys, i.e. Ti6Al4V alloy (6.020 Al, 4.10 V, 0.168 Fe, 0.160 O, 0.043 C and balanced Ti, mass fraction, %) and Ti6Al7Nb alloy (5.88 Al, 6.65 Nb, 0.03 Fe, 0.10 C, 0.20 O, 0.07 N, 0.02 H and balanced Ti). The surfaces were polished to a roughness of 0.04 μm. The main mechanical properties of the specimens are listed in Table 1. The artificial saliva (0.4 g NaCl, 0.4 g KCl, 0.795 g $CaCl_2{\cdot}2H_2O$, 0.78 g $CaCl_2{\cdot}2H_2O$, 0.005 g $Na_2S{\cdot}9H_2O$, 1 g urea, 100 g distilled water) was used to simulate the oral environment.

Fretting tests were performed under laboratory control conditions (temperature 23 °C; relative humidity 60%±10%). Maximum cyclic forces ($F_{max}$) were 200 and 400 N. To keep contact and avoid impact effect during testing, a minimum force ($F_{min}$) of 50 N was imposed for all tests. The speed of piston movement was controlled at 6 mm/min. The number of cycles was ranged from 1 to $10^4$. Prior to the tests, all specimens were ultrasonically cleaned in acetone. The morphologies of the damaged scars were examined by an optical microscope (OM, OLYMPUS BX60MF5) and a scanning electron microscope (SEM, JSM-6610LV) after the tests.

## 3 Results and discussion

### 3.1 Kinetic behavior

Figure 2 shows the effect of the inclined angle ($\theta$=45° and 60°) on the $F$−$D$ curves. At a lower inclined angle ($\theta$=45°), the shape of $F$−$D$ curve was ellipse at the initial stage, as shown in Fig. 2(a). With the increase of the number of cycles, the $F$−$D$ curves became quasi-

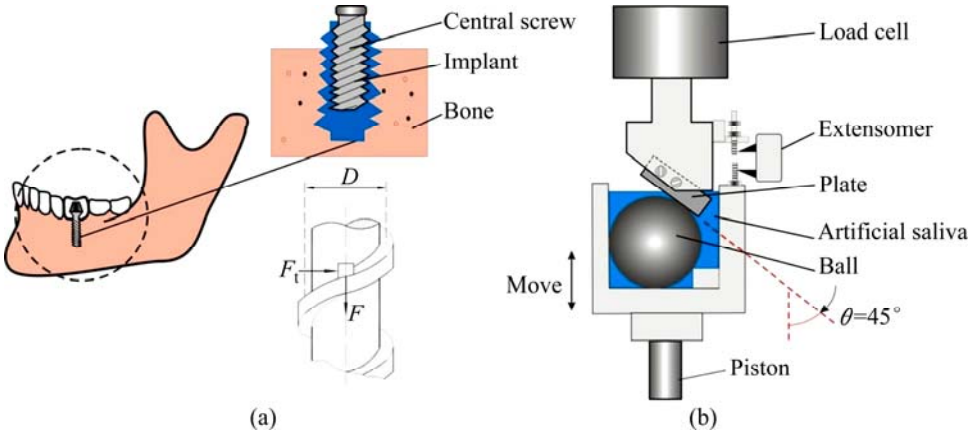


**Fig. 1** Schematic diagram of dual motion fretting wear test rig: (a) Dental implant; (b) Fretting device

**Table 1** Mechanical properties of specimens

| Sample | Yield strength/MPa | Ultimate tensile strength/MPa | Hardness (HV) |
|---|---|---|---|
| TA2 | 172 | 692 | 206 |
| Ti6Al7Nb | 730 | 950 | 342 |
| Ti6Al4V | 860 | 930 | 330 |

trapezoid as shown in Fig. 2(c). After about 500 cycles, narrow parallelogram $F-D$ curves can be observed (Fig. 2(d)). At the end, the $F-D$ curves appeared narrow parallelogram. For a large inclined angle of 60°, the $F-D$ curves changed from the initial narrow ellipse to the ended line.

Under a higher inclined angle ($\theta$=60°), all cycles corresponding to the shape of ellipse and line, which implied that the relation motion of contact surface was accommodated by elastic-plastic deformation and elastic deformation, respectively. It indicated that the fretting running state was partial slipping from the start to the end under $\theta$=60°. However, if $\theta$=45°, the kinetic curves always were in quasi-trapezoid shape after the initial stage (running-in stage), which indicated the fretting running in the state of gross slipping. From Fig. 2, it can

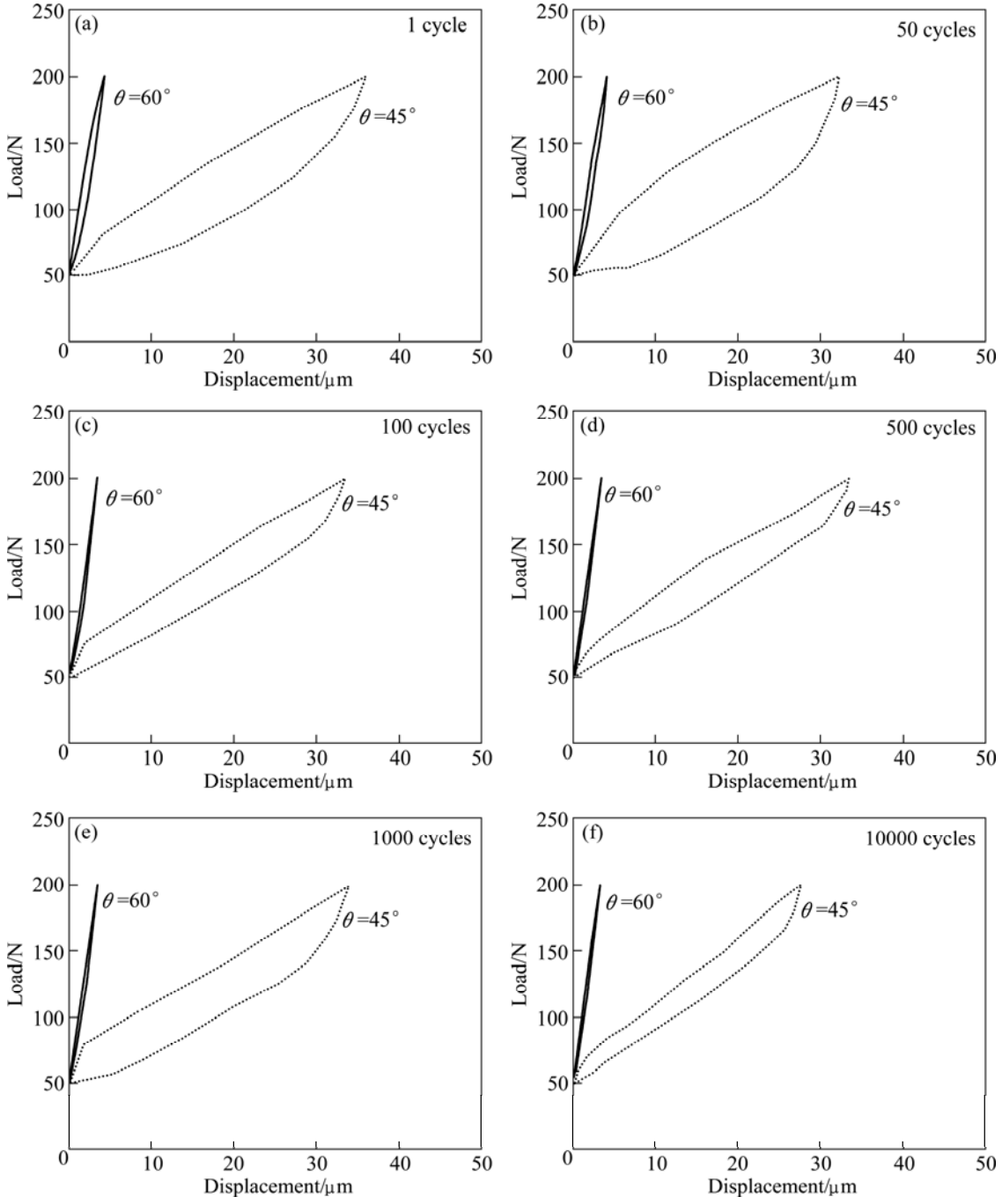


**Fig. 2** Variation of $F-D$ curves of Ti6Al7Nb/Ti6Al4V as function of number of cycles under inclined angles $\theta$ of 45° and 60° under $F_{max}$=200 N

be found that the radial displacement of the dual motion fretting reduced greatly with the increase of the inclined angle. At the same time, the area surrounded by the $F-D$ curve (i.e. dissipated energy during each cycle) also decreased greatly with the increase of the inclined angle. Therefore, the fretting running behavior of dual motion fretting strongly depended upon the inclined angle. The appearance of the wear debris can obviously change the surface situation of the contact interface, which is a import reason of the changes in the loop shape. To extend to the design of dental implants, the structure of the screw is very important.

Figure 3 shows the effect of materials on the dual motion fretting. For the TA2/Ti6Al4V contact-pair, the $F-D$ curve was in quasi-trapezoid shape like parallelogram before 1000 cycles, and the shape of the $F-D$ curve gradually transformed to ellipse at the end of the test (1000 cycles, see Fig. 3(f)). And the relative displacement was become smaller with the increase of cycles. It revealed that the fretting running state changed from gross slipping to partial slipping. For the Ti6Al7Nb/Ti6Al4V contact-pair, the shape was quasi-trapezoid from start to the end of the test, which corresponded to the fretting running in the state of gross slipping. Thus, the material characters strongly affected the kinetic behavior of dual motion fretting.

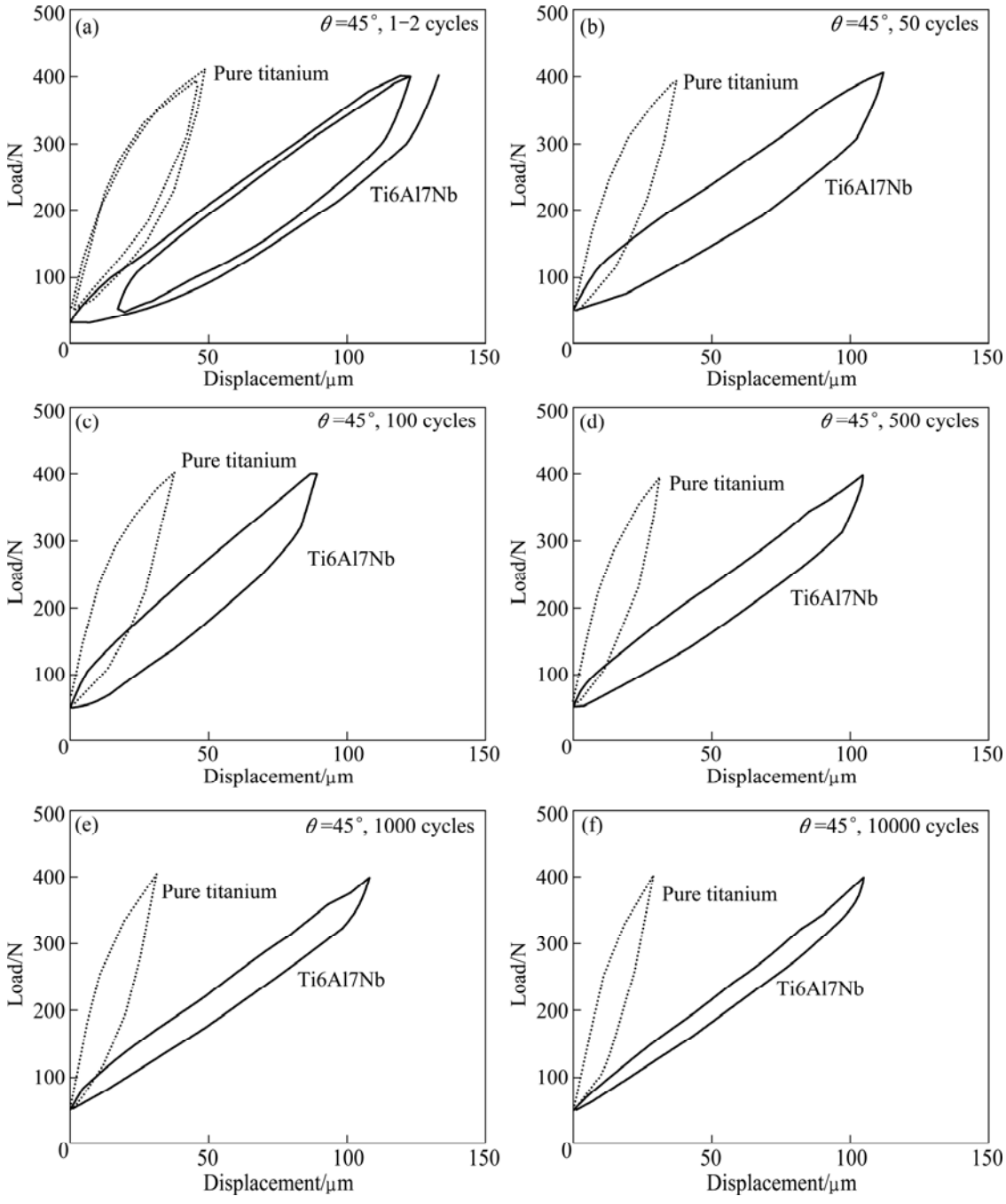


**Fig. 3** Variation of $F-D$ curves as function of number of cycles for different contact-pairs under $F_{max}$=400 N

Figure 4 shows the radial displacements under different imposed loads and inclined angles. It can be found that with the increase of the inclined angle and cycles, the relative displacement dropt down greatly, especially in the initial stage. There may be two reasons: firstly, under higher inclined angle, the radial component of dual motion fretting increased while tangential component decreased; secondly, the plastic deformation occurred mainly at the initiated stage and tended to the shakedown limit of plastic deformation. In other words, the radial displacement quickly reached the stable value, i.e. shakedown limit. At low inclined angle ($\theta$=45°), compared with TA2, the Ti6Al7Nb alloy has a high displacement and the procedure reached the steady stage which was longer than that of TA2 (Fig. 5). It may be the reason that Ti6Al7Nb had a better performance of anti-plastic flow, which induced the fretting difficultly transformed from the dual motion fretting to radial fretting [12,17]. However, at high inclined angle of 60°, the radial displacement of Ti6Al7Nb alloy was lower than that of TA2 alloy, which may be due to its higher contact stiffness. The high contact stiffness of Ti6Al7Nb was owing to its high hardness.

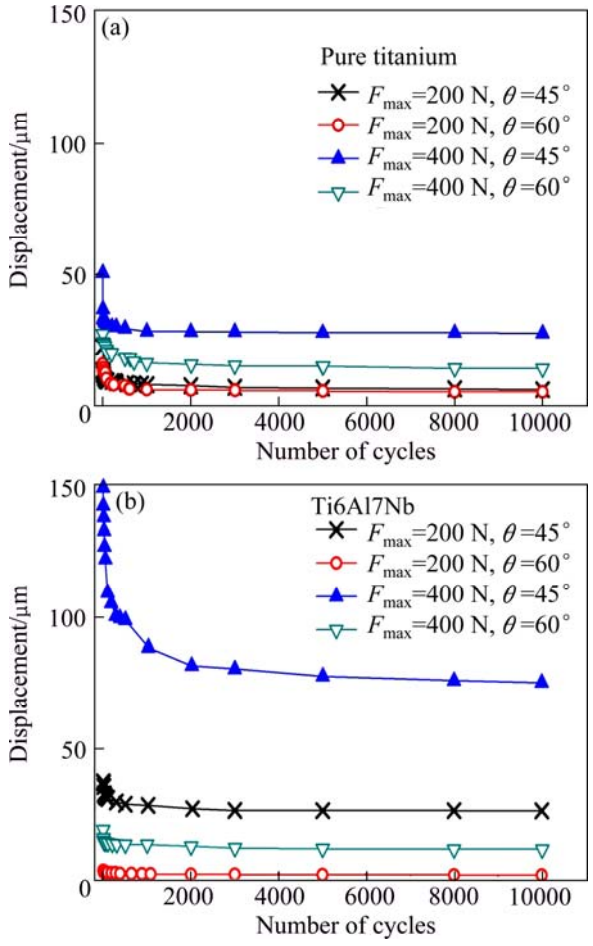


**Fig. 4** Evolutions of radial displacement as function of number of cycles

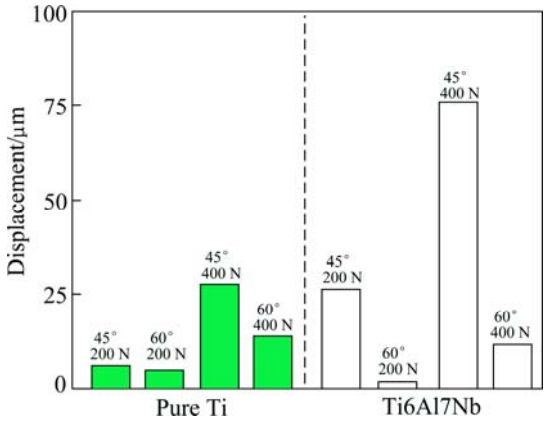


**Fig. 5** Stable radial displacement under different imposed loads (200 N, 400 N) and inclined angles (45°, 60°)

### 3.2 Damage observations

SEM morphologies of the worn scars of dual motion fretting are shown in Fig. 6. It can be found that the surface damage morphologies were asymmetric, and the severer wear was located at one side of the higher contact stress, which corresponded to the maximum imposed load. The fretting cracks nucleated and propagated mainly at the side with the higher imposed load. A transformation of fretting mode from the dual motion to the radial fretting mode may explain this phenomenon [12,17]. And the electrochemical corrosion traces were observed obviously on the other side of the scar. The wear increased accordingly with the increase of the imposed load and the decrease of the inclined angle. Meanwhile, when the inclined angle increased from 45° to 60°, the length of the wear scar decreased clearly. The worn scar became large when the inclined angle increased under the same imposed load, as shown in Figs. 6(e) and (f); also it became large when the imposed load increased at the same inclined angle, as shown in Figs. 6(a)−(d). It obviously shows that the worn scar in Fig. 6(b) is larger than that in Fig. 6(d). It can conclude that the damage extent of TA2 was severer than that of Ti6Al7Nb alloy under the same inclined angle and imposed load, namely, the Ti6Al7Nb alloy was more wear resistant than TA2 under the condition of dual motion fretting. The process of fretting corrosion needs a long term cycle, so the influence of corrosion is not obvious, and it cannot reflect the characteristics of the material to resist corrosion.

The cyclic plastic deformation accumulation, wear and cracking were dominant for the dual motion fretting damage. The subsequent 3D morphologies and profile measurements of fretting scars and their cross-sections also show that the surface damage was asymmetric, and the wear was located at one side of the higher imposed load. As shown in Figs. 7(a) and (b), at one side of the

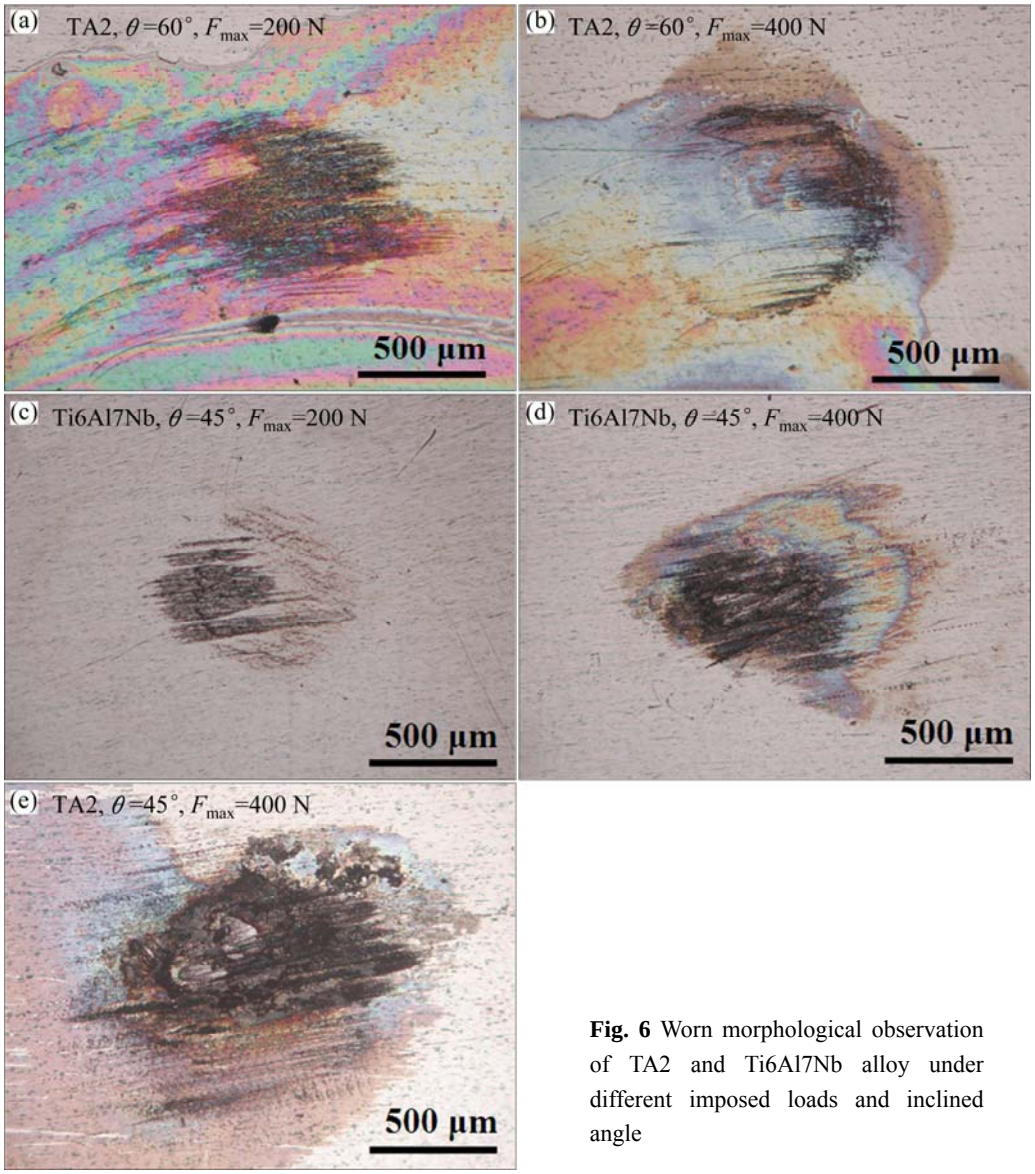


**Fig. 6** Worn morphological observation of TA2 and Ti6Al7Nb alloy under different imposed loads and inclined angle

worn scar, the 3D morphology presented a deep pit; however, on the other side of the worn scar, the 3D morphology was very rough with a great deal of debris accumulated (Figs. 7(a) and (c)). From Figs. 7 and 8, it is clearly shown that the Ti6Al7Nb alloy presented the better wear resistance than TA2, which indicated the Ti6Al7Nb alloy had a better potential application than TA2 in dental implants. The SEM morphologies (Fig. 9) indicated that some plastic flow traces, ploughing and spalling occurred in the worn scars. Combined the OM observation and the EDX analysis of the worn scar, it can summarize that the wear mechanisms of pure titanium TA2 and Ti6Al7Nb alloy were main abrasive wear, oxidative wear and delamination under the condition of dual motion fretting wear in artificial saliva.

## 4 Conclusions

1) The dual motion fretting wear tests with contacts of Ti6Al4V ball against TA2 and Ti6Al7Nb flats in artificial saliva have been carried out. The dual motion fretting kinetic and wear behaviors of TA2 pure titanium and Ti6Al7Nb alloy strongly depend upon the imposed load, inclined angle, the number of cycles and material properties. During the process of the dual motion fretting, the fretting running mode gradually transformed from the dual motion fretting to radial fretting, namely, the tangential fretting component reduced and the radial fretting component increased.

2) The Ti6Al7Nb presented better dual motion fretting wear resistance than TA2 in artificial saliva at the same test parameters. With the increase of inclined angle and decrease of imposed load, the wear extent became slight.

3) The wear mechanisms of pure titanium TA2 and Ti6Al7Nb alloy under the condition of dual motion fretting in artificial saliva were abrasive wear, oxidative wear and delamination.

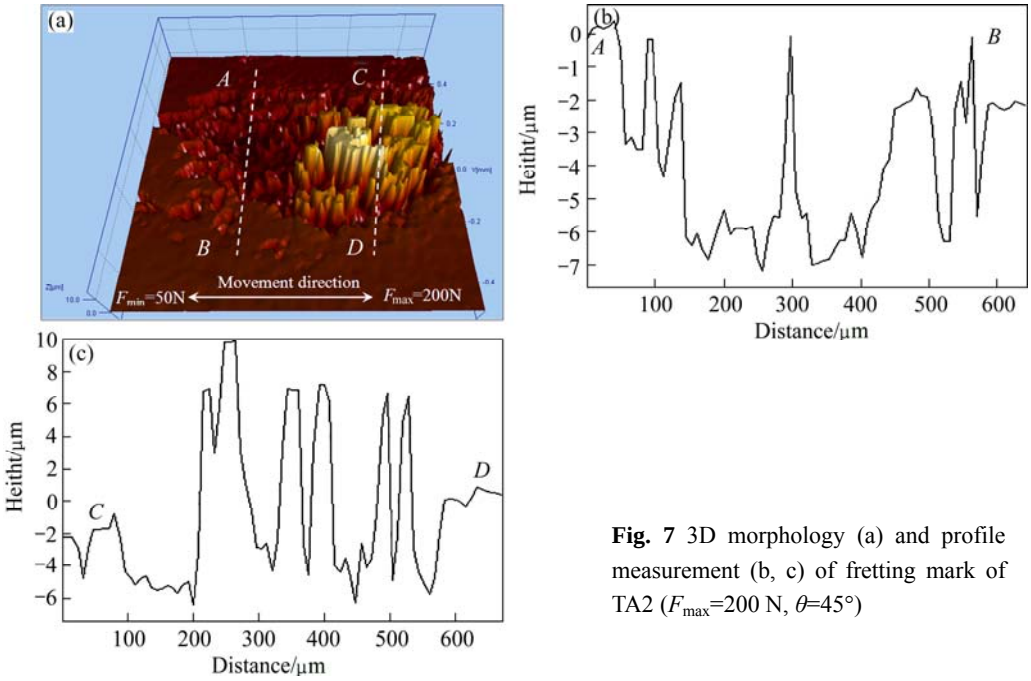


**Fig. 7** 3D morphology (a) and profile measurement (b, c) of fretting mark of TA2 ($F_{max}$=200 N, $\theta$=45°)

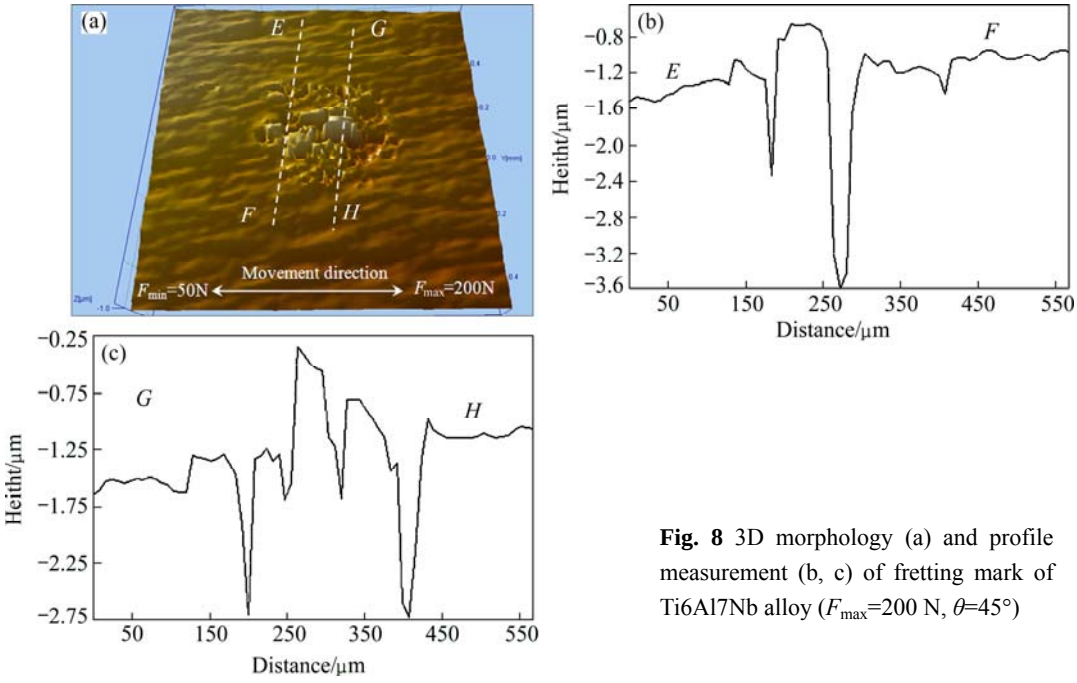


**Fig. 8** 3D morphology (a) and profile measurement (b, c) of fretting mark of Ti6Al7Nb alloy ($F_{max}$=200 N, $\theta$=45°)

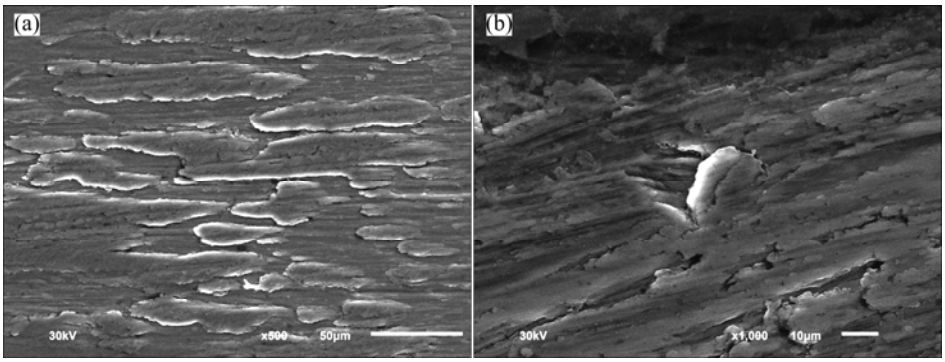


**Fig. 9** SEM images of fretting marks of Ti6Al7Nb alloy ($\theta$=45°): (a) $F_{max}$=200 N; (b) $F_{max}$=400 N

## References


[1] SONES A D. Complications with osseointegrated implants [J]. J Prosthet Dent, 1989, 62: 581−585.

[2] YOKOYAMA K, ICHIKAWA T, MURAKAMI H, MIYAMOTO Y, ASAOKA K. Fracture mechanisms of retrieved titanium screw thread in dental implant [J]. Biomaterials, 2002, 23: 2459−2465.

[3] ZHU M H, CAI Z B, LI W, YU H Y, ZHOU Z R. Fretting in prosthetic devices related to the human body [J]. Tribology International, 2009, 42: 1360−1364.

[4] YU H Y, CAI Z B, ZHOU Z R, ZHU M H. Fretting behavior of cortical bone against titanium and its alloy [J]. Wear, 2005, 259(7−12): 910−918.

[5] GAO S S, CAI Z B, QUAN H X, ZHU M H, YU H Y. Comparison between radial and dual-motion fretting features of cortical bone [J]. Tribology International, 2010: 440−446.

[6] YU H Y, GAO S S, CAI Z B, QUAN H X, ZHU M H. Dual-motion fretting behavior of mandibular cortical bone against pure titanium [J]. Tribology International, 2009, 42: 1365−1372.

[7] TOMOYA G, YOSHINOBU M, JOANNE N W, MICHAELL M. Fracture incidence in mandibular overdentures retained by one or two implants [J]. The Journal of Prosthetic Dentistry, 2010, 103: 178−181.

[8] SIVAKUMAR B, SATENDRA K, SANKARA T S N. Fretting corrosion behaviour of Ti6Al4V alloy in artificial saliva containing varying concentrations of fluoride ions [J]. Wear, 2011, 270: 317−324.

[9] BARRY M, KENNEDY D, KEATING K, SCHAUPERL Z. Design of dynamic test equipment for the testing of dental implants [J]. Materials and Design, 2005, 26: 209−216.

[10] JAARDA M J, RAZZOOG M E, GRATTON D G. Effect of preload torque on the ultimate tensile strength of implant prosthetic retaining screws [J]. Implant Dent, 1994, 3: 17−21.

[11] KIM S G, PARK J U, JEONG J H, BAE C, BAE T S, CHEE W. In vitro evaluation of reverse torque value of abutment screw and marginal opening in a screw-and cement-retained implant fixed partial denture design [J]. Int J Oral Maxillofac Implants, 2009, 24(6): 1061−1067.

[12] ZHU M H, ZHOU Z R. Dual-motion fretting wear behaviour of 7075 aluminium alloy [J]. Wear, 2003, 255: 269−275.

[13] CAI Z B, GAO S S, ZHU M H, LIU J, SHEN H M, YU H Y, ZHOU Z R. Investigation of micro-cracking behaviors of human femur cortical bone during radial fretting [J]. Tribology International, 2011, 44(11): 1556−1564.

[14] ZHOU Z R, VINCENT L. Fretting wear [M]. Beijing: Science Press, 2002.

[15] CAI Z B, ZHU M H, LIN X Z. Friction and wear of 7075 aluminum alloy induced by torsional fretting [J]. Transactions of Nonferrous Metals Society of China, 2010, 20: 371−376.

[16] LI J L, MA X X, SUN M G, SONG Z L. Structure and tribological performance of helium-implanted layer on Ti6Al4V alloy by plasma-based ion implantation [J]. Nuclear Instruments and Methods in Physics Research B, 2009, 267: 482−486.

[17] ZHU M H, ZHOU Z R, KAPSA P H, VINCEN T L. An experimental investigation on composite fretting mode [J]. Tribology International, 2001, 34(11): 733−738.


# 纯钛和钛合金在人工唾液中的复合微动磨损行为


张保荣[1,2]，蔡振兵[3]，甘雪琦[1]，朱旻昊[3]，于海洋[1]

1. 四川大学 口腔疾病研究国家重点实验室，成都 610041；

2. 航空总医院 口腔科，北京 100012；

3. 西南交通大学 材料先进技术教育部重点实验室 摩擦学研究所，成都 610031



**摘 要**：在改进后的液压伺服双向微动磨损试验机上实现双向微动。在人工唾液环境中，对 TA2 纯钛和 Ti6Al7Nb 合金在 6 mm/min 的加载速度下以不同接触倾角(45°和 60°)和不同最大外加载荷(200~400 N)条件下进行复合微动磨损实验。详细研究循环垂向力和倾斜角的影响。结合动力学分析与微观检测结果显示：磨痕和塑性变形累积呈现强烈的非对称性。在人工唾液环境中和相同实验参数下，Ti6Al7Nb 合金比 TA2 纯钛具有更好的抗磨损性能，并随着倾斜角度的增加和外加载荷的降低，磨损相应减轻。TA2 纯钛和 Ti6Al7Nb 合金在人工唾液环境中的复合微动磨损机制是磨粒磨损、氧化磨损和剥层。



**关键词**：钛合金；微动磨损；双向复合微动；切向微动；径向微动；磨损机理

**(Edited by Chao WANG)**